J Hepatobiliary Pancreat Sci (2012) 19:289–296
DOI 10.1007/s00534-011-0483-5

ORIGINAL ARTICLE

Morphometric and immunohistochemical study of cholangiolocellular carcinoma: comparison with non-neoplastic cholangiole, interlobular duct and septal duct

Sawako Maeno · Fukuo Kondo · Keiji Sano · Tadahiro Takada · Takehide Asano

Published online: 17 December 2011

Abstract
Background/purpose The origin of cholangiolocellular carcinoma (CoCC) is still controversial. To solve this problem, morphometric and immunohistochemical features of CoCC were examined.
Materials and methods Cancerous ducts: 15 CoCC lesions from 13 resected and two autopsied cases. Non-neoplastic ducts: 20 specimens of non-cancerous areas of eight resected CoCC cases and of 12 resected hepatocellular carcinoma (HCC) cases. From these specimens, cholangioles, interlobular ducts of small size (ILD-S), interlobular ducts of medium size (ILD-M) and septal ducts were randomly selected.
Morphometry The outer and inner diameters of these ducts were measured. Immunohistochemistry: two hepatocyte markers [Hep Par 1 and α-fetoptotein (AFP)], two cholangiocyte markers (cytokeratin CK7, CK19), a marker for mucin (Muc1), a hepatic stem/progenitor cell marker (c-Kit) and epithelial membrane antigen (EMA) were used.
Results Morphometry: both mean values of the outer and inner diameters of CoCC were far larger than those of cholangioles, and showed intermediate values between those of ILD-S and ILD-M. Immunohistochemistry: all ducts of CoCCs were negative for the two hepatocyte markers and positive for CK 7. Most CoCC ducts were positive for CK 19. Positive rate of c-Kit of cholangiole was most remote from that of CoCC. The positive rates of EMA in the membranous area of ducts were similarly very high in CoCC, cholangiole and ILD-S.
Conclusion These results suggest that CoCCs may originate from ILDs.

Keywords Cholangiolocellular carcinoma · Cholangiole · Interlobular duct · Morphometry · Immunohistochemistry

Introduction

Cholangiolocellular carcinoma (CoCC) is a unique primary liver cancer first reported by Steiner et al. [1]. Its histological features consist of small cancer glands resembling cholangioles. Formerly, this tumor had been categorized as a subtype of intrahepatic cholangiocarcinoma (ICC) [2], but it is now considered a different entity from ICC [3, 4]. Owing to the recent progress in studies of hepatic stem or progenitor cells, these stem/progenitor cells are thought to exist within or around cholangioles. CoCC is now speculated to originate from the cholangiole [5–7], although Steiner et al. [1] suggested an interlobular duct origin as well as cholangiole origin. CoCCs usually show different clinical features and images from the common cases of ICC [8–10]. Their images usually show mass forming type without dilatation of peripheral bile ducts. They sometimes develop in patients with chronic liver diseases.

In the present study, we examined the morphometric and immunohistochemical features of CoCCs and compared them with those of various non-neoplastic ducts [cholangioles, interlobular ducts (ILDs) and septal ducts] in order to clarify the cell origin.

S. Maeno · K. Sano · T. Takada
Department of Surgery, Teikyo University, School of Medicine, Tokyo, Japan

S. Maeno · F. Kondo (✉)
Department of Pathology, Teikyo University, School of Medicine, 2-11-1 Kaga, Itabashi-ku, Tokyo 173-8605, Japan
e-mail: fkondo55@coffee.ocn.ne.jp

T. Asano
Clinical Research Center, National Hospital Organization Chiba East Hospital, Chiba, Japan

Table 1 Clinico-pathological data of cholangiolocellular carcinoma cases

No. of cases	15
Age	46–86 years old (mean 65.1 years)
Gender	Male 8 patients, female 7 patients
Causative factors of liver diseases	HBsAg 2 cases, HCAb 4 cases, ALD 1 case
Specimen	Resection 13 cases, autopsy 2 cases
Non-cancerous liver tissue	NL 5 cases, CH 7 cases, LC 3 cases
No. of tumors	Solitary 14 cases, multiple 1 cases (3 tumors 1 case)
Tumor size	8–75 mm (mean 31.5 mm)
Cell differentiation	Well differentiated tubular adenocarcinoma 15 cases

HBsAg Hepatitis B surface antigen, *HCAb* hepatitis C antibody, *ALD* alcoholic liver disease, *NL* normal liver, *CH* chronic hepatitis, *LC* liver cirrhosis

Table 2 Clinico-pathological data of control cases

No. of cases	20 (CoCC 8 cases, HCC 12 cases)
Age	46–85 years old (mean 69.7 years)
Gender	Male 13 patients, female 7 patients
Causative factors of liver diseases	HBsAg 3 case, HCAb 10 cases
Specimen	Resection 20 cases
Non-cancerous liver tissue	NL 7 cases, CH 11 cases, 2 cases

CoCC Cholangiolocellular carcinoma, *HCC* hepatocellular carcinoma, *HBsAg* hepatitis B surface antigen, *HCAb* hepatitis C antibody, *NL* normal liver, *CH* chronic hepatitis, *LC* liver cirrhosis

Materials and methods

Materials

A total of 15 CoCC lesions from 13 resected and two autopsied cases were retrieved from the histopathology files of the Teikyo University Hospital and consultation files of the Department of Pathology of Teikyo University, during the period of 1990–2011. As control tissue for comparative study, 20 specimens of non-cancerous areas consisting of eight resected CoCC cases and 12 resected hepatocellular carcinoma (HCC) cases were also retrieved from the same histopathology files.

Clinico-pathological data

Clinico-pathological data of the CoCC and control cases are shown in Tables 1 and 2. The CoCC cases ranged in age from 46 to 86 years (mean 65.1 years), and eight were male and seven female. As to the causative factors of liver disease, two patients were positive for hepatitis B surface antigen (HBsAg), four for hepatitis C antibody (HCAb), and one had alcoholic liver disease. Histological features of non-cancerous extra-nodular liver tissue showed normal liver in five cases, chronic hepatitis in seven cases and liver cirrhosis in three cases. Fourteen cases had solitary tumors and one had 3 tumors. In this study, only the largest tumors were examined. The large diameters of these 15 tumors ranged from 0.8 to 7.5 cm (mean 3.15 cm). Microscopically, all 15 tumors showed histological features of well-differentiated tubular adenocarcinoma (Fig. 1).

Patient age of the control cases ranged from 46 to 85 years (mean 69.7 years) (Table 2). Thirteen patients were male and seven were female. Three were positive for HBsAg and 10 for HCAb. All 20 were resected cases. Non-cancerous extra-nodular liver tissues were normal liver in seven cases, chronic hepatitis in 11 cases and liver cirrhosis in two cases.

Methods

Classification of glands

The diagnosis of CoCC was based on the definitions described in the newest version of WHO classification of tumors of the digestive system [3] and the general rules for the clinical and pathological study of primary liver cancer (5th edition, revised version) [4]. The non-neoplastic ducts were classified according to the description of previous works [11, 12].

Cholangioles: small ducts located at peripheral areas (a little outside) of portal tracts without accompanying portal veins and arteries (Fig. 1a, b). Interlobular ducts and septal ducts: ducts located at the central area of portal tracts accompanying portal veins and arteries. Ducts thinner than 100 μm were classified as ILDs (Fig. 1a–d), and those thicker than 100 μm were classified as septal ducts (Fig. 1e). ILDs were subclassified as ILDs of small size (ILD-S, thinner than 40 μm) and ILDs of medium size (ILD-M, thicker than 40 μm), according to the definition [12, 13]. From these control specimens, 321 cholangioles, 382 ILD-Ss, 180 ILD-Ms and 82 septal ducts were randomly selected. From the CoCC cases, a total of 1500 ducts (100 ducts/case) were also randomly selected.

Morphometry

Using the image analysis software Image J (National Institutes of Health, Bethesda, MD, USA) [13], the outer

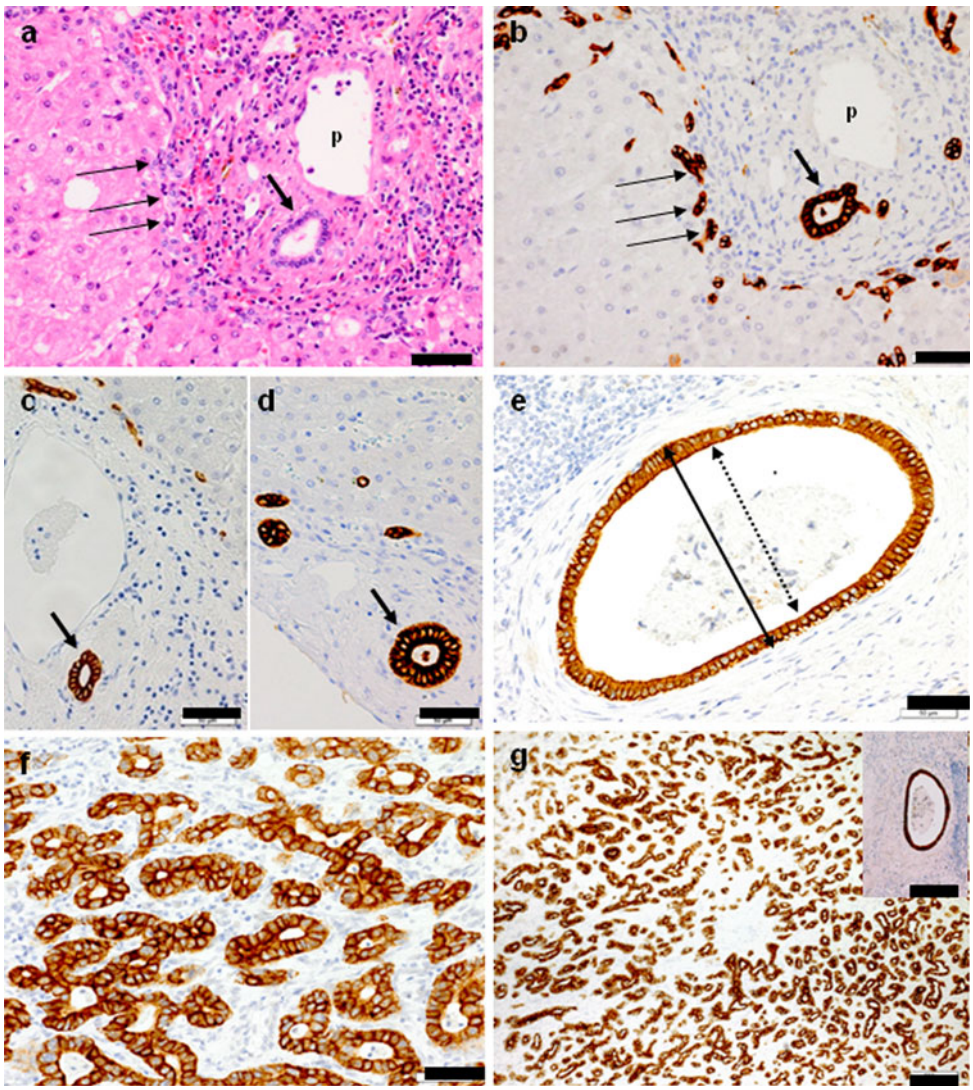

Fig. 1 Classification of various ducts. **a** HE stain, **b–g** CK7 immunostain. *Bar* 50 μm (**a–f**), *bar* 200 μm (**g** and *inset*). **a** Cholangioles (*thin arrows*), interlobular duct (*thick arrow*) and portal vein (*p*). **b** CK7 immunostain of the same specimen as **a**. Cholangioles locate at peripheral areas (a little outside) of portal tracts without accompanying portal veins. An interlobular duct (ILD) is located at the central area of portal tracts accompanying a portal vein. **c** An interlobular duct of small size (ILD-S) thinner than 40 μm (*arrow*). **d** An interlobular duct of medium size (ILD-M) thicker than 40 μm (*arrow*). **e** A septal duct thicker than 100 μm. *Arrows* with *solid line* and *arrows* with *dashed line* show outer and inner diameters, respectively. **f** Ducts of cholangiolocellular carcinoma (CoCC). Cancer ducts show a tubular, cord-like, anastomosing pattern, the so-called antler-like pattern. **g** A low magnification view of ducts of CoCC and a septal duct (*inset* the same duct as **e**). In comparison with the septal duct, ducts of CoCC look very thin

and inner diameters of these ducts were measured in the minor axis direction on digital photographs of CK7 immunostaining (Fig. 1e). Based on the morphometric data, sample minimum, lower quartile, mean, upper quartile, and sample maximum were computed to make box-and-whisker diagrams (boxplots) (Figs. 2, 3).

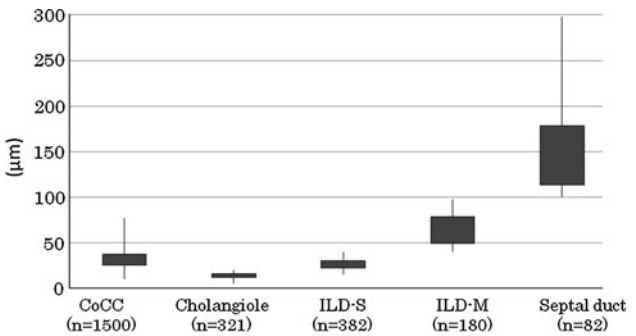

Fig. 2 Outer diameter of cholangiolocellular carcinoma ducts and control ducts

Immunohistochemistry

Tissue samples were fixed with 10% formalin, embedded in paraffin, and then sliced at 4 μm. In addition to hematoxylin-eosin (HE) staining, immunohistochemical study was performed on paraffin sections with the antibodies listed in Table 3. Two hepatocyte markers [Hep Par 1 and α-fetoptotein (AFP)], two cholangiocyte markers (cytokeratin CK7, CK19), a marker for mucin (Muc1), a hepatic stem/progenitor cell marker (c-Kit) and epithelial membrane antigen (EMA) were used. In the cases showing positive staining with Muc1, diastase digested periodic acid-Schiff (PAS) staining and alcian blue staining were performed. For each marker, stainability (positively or negatively stained) was evaluated. A quantitative evaluation of positive cells was not done because the cell number within a duct was very small. Even when the case showed only a few positive cells, it was classified as positive. Using

c-Kit, one positive cell within a duct was sufficient for positive evaluation. Concerning EMA, stain patterns were classified into membranous pattern and cytoplasmic pattern based on the positive area in the duct. When both membranous area and cytoplasm were positively stained, this pattern was classified as membranous pattern because positivity was usually more intense in the membranous area than in the cytoplasm.

Statistical analysis

In order to compare the outer and inner diameters of various ducts, *t* test was used. For comparison of the positive rates of various antibodies, chi-square test was used. p value <0.05 was recognized as significant.

Results

Morphometry

Outer diameter of glands of CoCC and control ducts

Range (sample minimum–sample maximum), mean, standard deviation (SD), p value in CoCC versus various duct groups were as follows, and a boxplot is shown in Fig. 2.

Cholangiolocellular carcinoma 10.2–76.6, 31.8, 9.2 μm

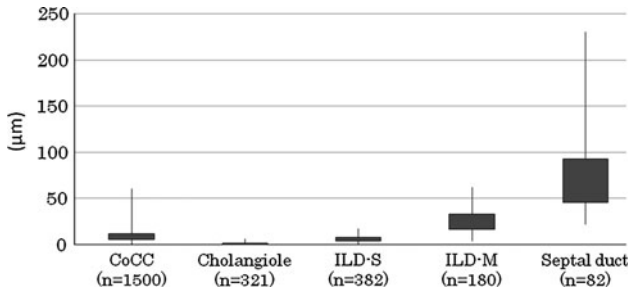

Fig. 3 Inner diameter of cholangiolocellular carcinoma ducts and control ducts

Cholangiole 5.4–19.7, 13.8, 3.0 μm, $p < 0.0001$
ILD-S 15.3–39.9, 26.5, 5.6 μm, $p < 0.0001$
ILD-M 40.4–97.7, 65.0, 17.3 μm, $p < 0.0001$
Septal duct 100.7–298.0, 149.9, 48.7 μm, $p < 0.0001$

The outer diameter of CoCC was far larger than that of cholangiole ($p < 0.0001$). It was also significantly larger than that of ILD-S ($p < 0.0001$) but significantly smaller than that of ILD-M ($p < 0.0001$) (Figs. 1a–d, f, 2). It was far smaller than that of septal duct ($p < 0.0001$) (Figs. 1e–g, 2).

Inner diameter of glands of cholangiolocellular carcinoma and control ducts

Range, mean, SD, p value versus CoCC in various duct groups were as follows, and the boxplot is shown in Fig. 3.

Cholangiolocellular carcinoma 0–60.6, 9.3, 5.9 μm
Cholangiole 0–6.1, 1.1, 1.2 μm, $p < 0.0001$
ILD-S 0.5–17.7, 6.5, 3.6 μm, $p < 0.0001$
ILD-M 4.1–62.0, 11.4, 24.7 μm, $p < 0.0001$
Septal duct 21.7–230.8, 76.7, 42.5 μm, $p < 0.0001$

The inner diameter of CoCC was far larger than that of cholangiole ($p < 0.0001$). It was also significantly larger than that of ILD-S ($p < 0.0001$). However, it was significantly smaller than that of ILD-M ($p < 0.0001$) (Figs. 1a–d, f, 2).

Immunohistochemistry

Hepatocyte markers: Hep Par 1 and AFP

Both Hep Par 1 and AFP were negatively stained in all ducts of CoCC and control ducts (Table 4). CoCC and

Table 3 List of antibodies and staining reagents

Primary antibody	Clone	Species	Reference	Dilution	Staining reagent
Hep Par 1	OCH1E5	Mouse	DAKO, Tokyo, Japan	1:60	DAB
AFP	C3	Mouse	Novocastra, Newcastle, UK	1:60	DAB
CK7	OV-TL12/30	Mouse	DAKO	1:60	DAB
CK19	RCK108	Mouse	MP Biomedicals, Morgan Irvine, CA, USA	1:60	DAB
Muc1	Ma695	Mouse	Novocastra	1:125	DAB
c-Kit		Rabbit	DAKO	1:125	DAB
EMA	E29	Mouse	DAKO	1:125	DAB

DAB Diaminobenzidene, *AFP* α-fetoprotein, *CK* cytokeratin, *EMA* epithelial membrane antigen

Table 4 Results of immunohistochemistry in cholangiolocellular carcinoma and control ducts

	Hep Par1	AFP	CK7	CK19	MUC1	c-Kit	EMA
CoCC ($n = 1500$)	0 (0%)	0 (0%)	1500 (100%)	1337 (89.1%)	103 (6.9%)	29 (1.9%)	1481 (98.7%) M: 1419 (94.6%) C: 62 (4.1%)
Cholangiole ($n = 321$)	0 (0%)	0 (0%)	321 (100%)	308 (96.0%)**	68 (21.2%)*	151 (47.0%)*	321 (100%) M: 321 (100%)* C: 0 (0%)
ILD-S ($n = 382$)	0 (0%)	0 (0%)	382 (100%)	360 (94.2%)**	116 (30.4%)*	52 (13.6%)*	382 (100%) M: 356 (93.2%)** C: 26 (6.8%)
ILD-M ($n = 180$)	0 (0%)	0 (0%)	180 (100%)	175 (97.2%)**	33 (18.3%)*	14 (7.8%)*	180 (100%) M: 22 (12.2%)* C: 158 (87.8%)
Septal duct ($n = 82$)	0 (0%)	0 (0%)	82 (100%)	80 (97.6%)**	21 (25.6%)*	4 (4.9%)	82 (100%) M: 0 (0%)* C: 82 (100%)

CoCC Cholangiolocellular carcinoma, *ILD-S* interlobular duct (small), *ILD-M* interlobular duct (medium-sized), *M* membrane-positive, *C* cytoplasm-positive versus cholangiolocellular carcinoma

* $p < 0.0001$, ** $p < 0.05$

control ducts did not show hepatocytic character immunohistochemically.

Cholangiocyte markers: CK7 and CK19

The cholangiocyte marker CK7 was positively stained in all ducts of CoCC and control ducts (Table 4; Fig. 1). CK19 was positively stained in most of the CoCC ducts and control ducts (Table 4). The positive rate in CoCC, cholangiole, ILD-S, ILD-M and septal ducts was 89.1, 96.0, 94.2, 97.2 and 97.6%, respectively. These results of CK7 and CK19 showed that CoCC and control ducts have cholangiocyte character.

Marker for mucin: Muc1

The positive rates of Muc1 in CoCC, cholangiole ILD-S, ILD-M and septal ducts were 6.9, 21.2, 30.4, 18.3 and 25.6%, respectively (Table 4; Fig. 4). The positive rate in CoCC was significantly lower than any control duct group ($p < 0.05$). Although the positive rate was low, some CoCCs did stain positive for Muc1. The positivity was confirmed by diastase digested PAS staining and alcian blue staining (Fig. 4).

Stem/progenitor cell marker: c-Kit

c-Kit was positively stained in 1.9% of CoCC ducts (Table 4; Fig. 5). However, cholangioles, ILD-Ss, ILD-Ms and septal ducts also showed positivity of 47.0, 13.6, 7.8 and 4.9%, respectively (Table 4). Among control ducts, the positive rate of cholangiole was farthest from that of CoCC.

Epithelial membrane antigen

Epithelial membrane antigen was positively stained in almost all CoCC ducts and in all control ducts. However, stain patterns (membranous or cytoplasmic pattern) were different depending on the ducts (Table 4; Fig. 6). CoCC ducts, cholangioles and ILD-Ss showed positive rates of membranous pattern of nearly or precisely 100%. However, thicker ducts, e.g., ILD-Ms and septal ducts, showed lower positive rates, 12.2 and 0%, respectively.

Stain patterns of EMA of control ducts showed a close relationship with duct size (outer diameter) (Fig. 7). Within the range from 5 to 54.9 μm, the smaller the duct size, the higher the positive rate of membranous pattern, and the lower the cytoplasmic pattern (Fig. 7). A transitional zone of stain patterns of EMA, roughly defined as 30–50 μm, and a conversion point at about 40 μm, was noted.

By contrast, the stain patterns of EMA of CoCC ducts were membranous pattern-dominant, independent of duct sizes (Fig. 8). In every size, the positive rate of membranous pattern was higher than 90%.

Discussion

Based on the recent advances in hepatic stem/progenitor cell research, some primary liver cancers are thought to

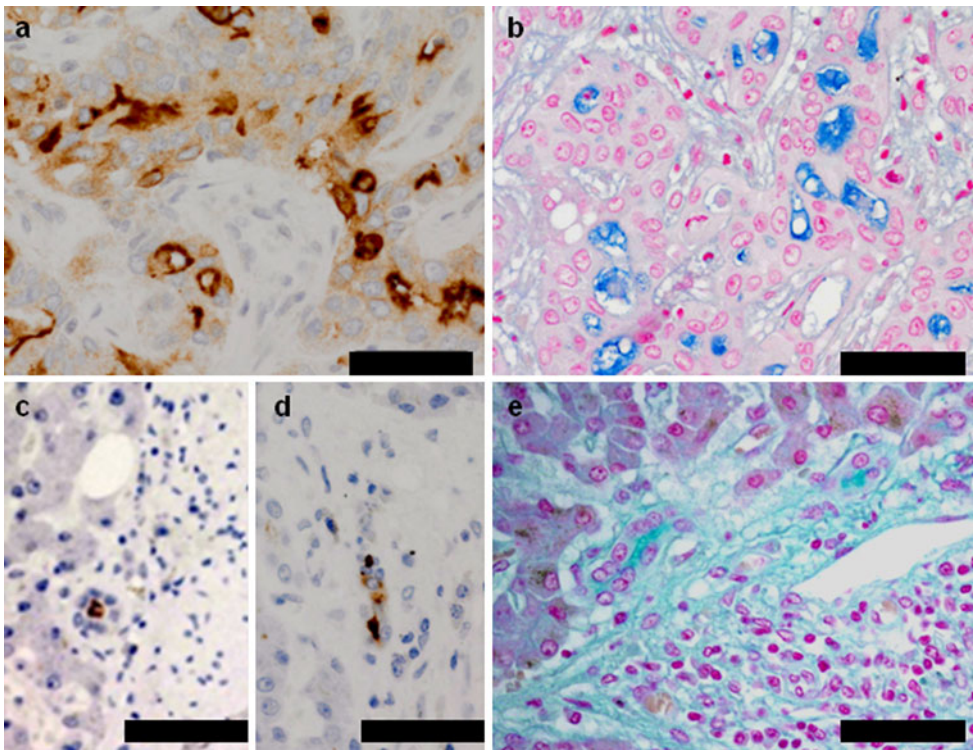

Fig. 4 Immunohistochemistry of Muc1 and alcian blue stain in CoCC and cholangiole. **a** Muc1-positive area of CoCC. Both glandular lumina and intracytoplasmic areas are positive for Muc1. **b** Alcian blue stain of the same area as **a**. Both glandular lumina and intracytoplasmic areas are positive for alcian blue. **c** A cholangiole positive for Muc1 in the glandular lumen. **d** A cholangiole positive for Muc1 in the glandular lumen and in the cytoplasm. **e** Other cholangioles positive for alcian blue in the glandular lumina. *Bar* 50 μm (**a**–**e**)

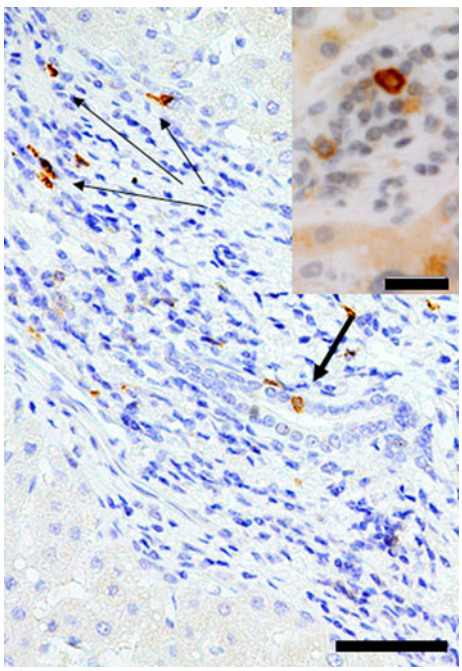

Fig. 5 Immunohistochemistry of c-Kit in cholangioles and an ILD. *Thin arrows* show c-Kit-positive cells in cholangioles. *Thick arrow* shows a c-Kit-positive cell in an ILD-S. This positive cell shows similar size and features to neighboring ILD cells except for the c-Kit positivity. *Bar* 50 μm. *Inset* shows high magnification view of c-Kit positive cells in cholangioles. *Bar* 20 μm

originate from such cells [14]. CoCC is speculated to arise from cholangioles, where these stem/progenitor cells exist [5–7], and thus is now classified as a different entity from ICC [3, 4]. However, interlobular ducts were also believed to be the origin of CoCC, since Steiner et al. [1] initially reported this unique tumor. In any event, the cell origin of CoCC has been a matter of debate until now.

In order to finally settle this controversy, we performed morphometric and immunohistochemical studies of CoCCs as well as various non-neoplastic ducts (cholangioles, interlobular ducts and septal ducts). We were able to obtain some useful findings as described below.

Duct size

Precise morphometric data of CoCC as well as control ducts were clarified for the first time in this study. Both the outer and inner diameters of CoCC were far larger than those of cholangioles, showing intermediate values between those of ILD-S and ILD-M. This was an unexpected result, suggesting interlobular bile duct to be the more likely origin of CoCC than cholangiole. In cases of poorly differentiated adenocarcinoma, both cell size and duct size may change variously. They can be far larger than those of the original benign ducts in some cases, and they can be far smaller in other cases. However, the well-differentiated tubular adenocarcinomas in the present study must not have shown extensive size alteration. According to our morphometric study of well- and moderately-differentiated adenocarcinoma of hepatic hilus (350 tumor cells from five cases), the tumor cells showed almost the same size as non-tumor cells (unpublished data). In our

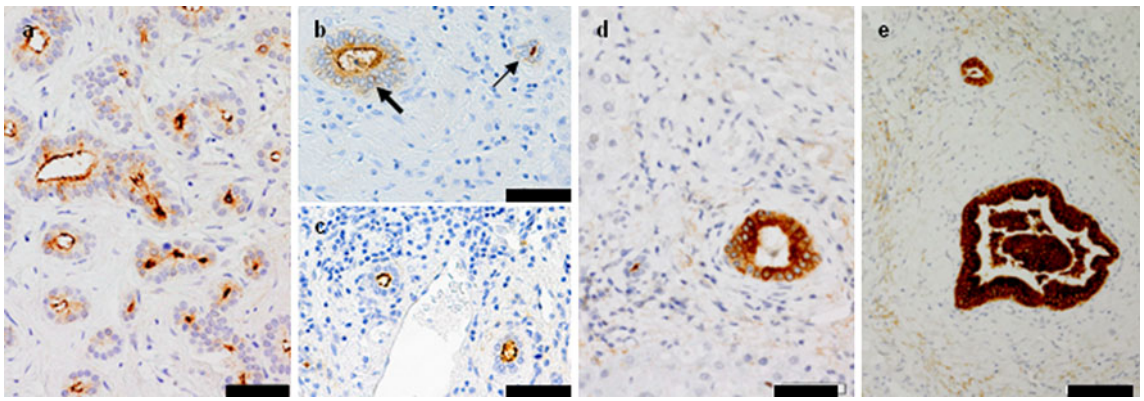

Fig. 6 Immunohistochemistry of EMA in CoCC and control ducts. **a** CoCC ducts mostly showed positive stain in the membranous areas of the lumina (membranous pattern). **b** A cholangiole (*thin arrow*) and an ILD-M (*thick arrow*) show membranous pattern. **c** Two ILD-Ss show membranous pattern. **d** An ILD-M shows positivity in the cytoplasm (cytoplasmic pattern). **e** A septal duct shows cytoplasmic pattern. *Bar* 50 μm (**a**–**d**), 100 μm (**e**)

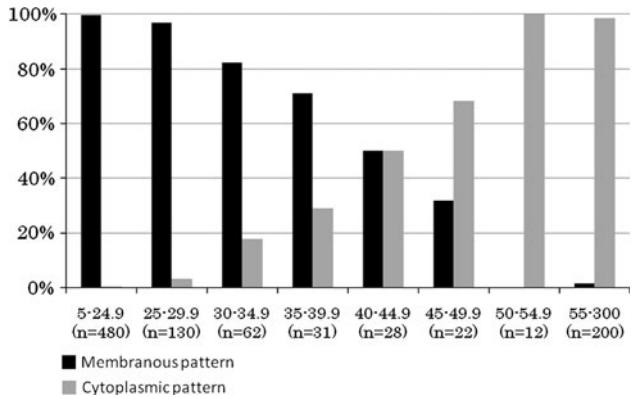

Fig. 7 Relationship between duct sizes and stain patterns of EMA in control ducts

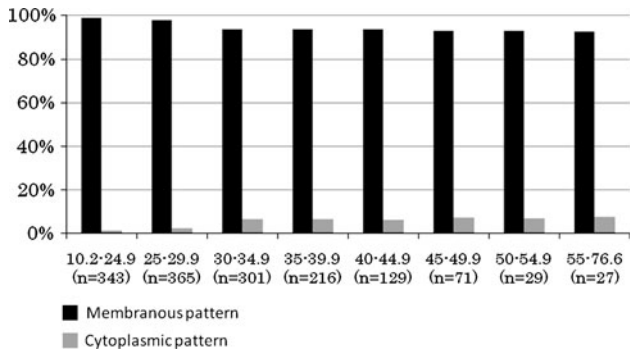

Fig. 8 Relationship between duct sizes and stain patterns of EMA in CoCC

morphometric study of HCC, well-differentiated HCC cells were smaller than non-cancerous hepatocytes [15]. In high magnification views (Fig. 1a–d, f), the CoCC duct is apparently far larger than the cholangiole, with its size appearing similar to ILDs. In a low magnification view (Fig. 1g), however, CoCC ducts look far thinner than septal ducts, providing a plausible explanation for the reason why many pathologists thought that CoCC resembles cholangiole.

Character of CoCC

All or nearly all CoCC ducts were stained negatively for hepatocyte markers and positively for cholangiocyte markers. This result showed that CoCC had cholangiocyte character but not hepatocyte character. Although the positive rate was low, Muc1 was positively stained in CoCC. This also suggests the adenocarcinoma character of CoCC.

As a matter of fact, it has been believed that CoCC does not show mucin production [3, 4]. However, cholangioles did show mucin production in the present study. Therefore, mucin production cannot be an exclusion item for the diagnosis of CoCC. Because the positive rate of mucin staining is far lower than control ducts, CoCC must have been recognized as carcinoma without mucin.

So far, MUC1–4, 5AC, 5B, 6–8, 11–13 and 15–17 genes coding the backbone mucin core protein have been identified in humans. Among these MUCs, we used MUC1 in the present study because this antibody was proved to be well sensitive for detecting mucin in the previous study [16]. We also used diastase digested PAS staining and alcian blue staining to exclude the possibility of false positive.

The positive rate of c-Kit (stem/progenitor cell marker) was far lower than that of cholangiole. Furthermore, c-Kit was positively stained in ILD-S, ILD-M and septal duct, suggesting that c-Kit is not a reliable specific marker for stem/progenitor cells. These results could not prove a stem/progenitor character of CoCC.

Stain patterns of EMA

The positive stain of EMA in the membranous site of the cancer duct (membranous pattern) has been recognized as a

specific feature of CoCC [17]. In fact, more than 90% of CoCC ducts showed a membranous pattern in this study. However, this result did not necessarily support the cholangiole origin theory of CoCC. Among various control ducts, not only cholangioles but also ILD-Ss and ILD-Ms showed a membranous pattern. A transitional zone was evident in the range of 30–50 μm, with the conversion point from membranous to cytoplasmic pattern being around 40 μm. These findings of the EMA staining pattern suggest that CoCC might have arisen from cholangioles or ILDs.

Finally, the clinical and imaging findings of CoCC should be discussed. CoCCs are frequently associated with chronic liver diseases. The images of CoCC usually show mass forming type without dilatation of peripheral bile ducts [9–11]. Such clinical and imaging findings can also be explained by the ILD origin theory. Because an ILD is the thinnest bile duct except for cholangioles and bile canaliculi, a carcinoma originating from an ILD cannot cause dilatation of peripheral bile ducts. That is why the carcinoma shows mass forming type in images. If chronic inflammation of peripheral portal tracts promotes carcinogenesis of cholangiocytes of ILDs, the co-existence of CoCC and chronic liver disease is reasonable.

Based on these findings and considerations, ILD is more likely to be considered as the origin of CoCC than cholangiole. The results and conclusions of this study differed from other studies. The former studies should also be respected. Because the morphometric and immunohistochemical findings may not be the direct evidence of interlobular duct carcinoma, more detailed molecular studies are necessary to clarify the origin of CoCC.

Acknowledgments We express sincere gratitude to Prof. Shinya Yoshino, Mr. Hitoshi Wakamatsu and Mr. Yuusuke, Morita, Department of Radiological Technology, Faculty of Medical Technology, Teikyo University, for their support in morphometric study. We also thank Mr. Masato Watanabe and Ms. Yurie Soejima, Department of Pathology for their technical contribution. This study was supported in part by the grants from The Vehicle Racing Commemorative Foundation.

Conflict of interest The authors declare that they have no conflict of interest.

References

1. Steiner PE, Higginson J. Cholangiolocellular carcinoma of the liver. Cancer. 1959;12:753–9.
2. Nakanuma Y, Leong ASY, Sripa B, Ponchon T, Vatanasapt V, Ishak KG. Intrahepatic cholangiocarcinoma. In: Hamilton SR, Altonen LA, editors. World health organization classification of tumors. Pathology and genetics of tumours of the digestive system. Lyon: International Agency for Research on Cancer; 2000. p. 173–80.
3. Theise ND, Nakashima O, Park YN, Nakanuma Y. Combined hepatocellular-cholangiocarcinoma. In: Bosman FT, Carneiro F, Hruban RH, Theise ND, editors. World health organization classification of tumors. WHO classification of tumors of the digestive system. Lyon: International Agency for Research on Cancer; 2010. p. 225–7.
4. Liver Cancer Study Group of Japan. The general rules for the clinical and pathological study of primary liver cancer. 5th ed. Revised version. Tokyo: Kanehara; 2009. p. 46.
5. Shiota K, Taguchi J, Nakashima O, Nakashima M, Kojiro M. Clinicopathologic study on cholangiolocellular carcinoma. Oncol Rep. 2001;8(2):263–8.
6. Komuta M, Spee B, Vander Borght S, De Vos R, Verslype C, Aerts R, et al. Clinicopathological study on cholangiolocellular carcinoma suggesting hepatic progenitor cell origin. Hepatology. 2008;47:1544–56.
7. Kozaka K, Sasaki M, Fujii T, Harada K, Zen Y, Sato Y, et al. A subgroup of intrahepatic cholangiocarcinoma with an infiltrating replacement growth pattern and a resemblance to reactive proliferating bile ductules: 'bile ductular carcinoma'. Histopathology. 2007;51:390–400.
8. Motosugi U, Ichikawa T, Nakajima H, Araki T, Matsuda M, Suzuki T, et al. Cholangiolocellular carcinoma of the liver: imaging findings. J Comput Assist Tomogr. 2009;33:682–8.
9. Asayama Y, Tajima T, Okamoto D, Nishie A, Ishigami K, Ushijima Y, et al. Imaging of cholangiolocellular carcinoma of the liver. Eur J Radiol. 2010;75:e120–5.
10. Fukukura Y, Hamanoue M, Fujiyoshi F, Sasaki M, Haruta K, Inoue H, et al. Cholangiolocellular carcinoma of the liver: CT and MR findings. J Comput Assist Tomogr. 2000;24:809–12.
11. Desmet VJ, Roskams T, De Vos R. Normal anatomy in gall bladder and bile ducts. In: LaRusso N, editor. Vol 6 of the series. Gastroenterology and Hepatology. The comprehensive visual reference. Philadelphia: Current Medicine; 1997. p. 1–29.
12. Roskams T, Desmet VJ, Verslype C. Development, structure and function of the liver. In: Burt AD, Portman BC, Ferrel LD, editors. MacSween's pathology of the liver. 5th ed. Philadelphia: Churchill Livingstone Elsevier; 2007. p. 1–73.
13. Abramoff MD, Magalhaes PJ, Ram SJ. Image processing with Image J. Biophotonics Int. 2004;11:36–42.
14. Theise ND, Yao JL, Harada K, Hytiroglou P, Portmann B, Thung SN, et al. Hepatic "stem cell" malignacies in adults four cases. Histopathology. 2003;43:263–71.
15. Kondo F, Wada K, Kondo Y. Morphometric analysis of hepatocellular carcinoma. Virchows Arch A Pathol Anat Histopathol. 1988;413:425–30.
16. Shibuya M, Kondo F, Sano K, Takada T, Asano T. Immunohistochemical study of hepatocyte, cholangiocyte and stem cell markers of hepatocellular carcinoma. J Hepatobiliary Pancreat Sci. 2011;18:537–43.
17. Nakano M. Histopathological characteristic of cholangiolocellular carcinoma. Tan To Sui (Biliary Tract and Pancreas). 2004;25:343–9. (in Japanese).